



Synthesis of indano[60]fullerene thioketone and its application in organic solar cells

Yong-Chang Zhai¹, Shimon Oiwa¹, Shinobu Aoyagi^{*2}, Shohei Ohno³, Tsubasa Mikie³, Jun-Zhuo Wang¹, Hirofumi Amada¹, Koki Yamanaka¹, Kazuhira Miwa¹, Naoyuki Imai⁴, Takeshi Igarashi⁴, Itaru Osaka³ and Yutaka Matsuo^{*1,5}

Letter

[Open Access](#)

Address:

¹Department of Chemical Systems Engineering, Graduate School of Engineering, Nagoya University, Furo-cho, Chikusa-ku, Nagoya 464-8603, Japan, ²Department of Information and Basic Science, Nagoya City University, Nagoya 467-8501, Japan, ³Applied Chemistry Program, Graduate School of Advanced Science and Engineering, Hiroshima University 1-4-1 Kagamiyama, Higashi-Hiroshima, Hiroshima 739-8527, Japan, ⁴Institute for Advanced Fusion, Resonac Corporation, 5-1 Okawa-cho, Kawasaki-ku, Kawasaki-shi, Kanagawa 210-0858, Japan and ⁵Institute of Materials Innovation, Institutes for Future Society, Nagoya University, Furo-cho, Chikusa-ku, Nagoya 464-8603, Japan

Email:

Shinobu Aoyagi^{*} - aoyagi@nsc.nagoya-cu.ac.jp; Yutaka Matsuo^{*} - matsuo.yutaka@material.nagoya-u.ac.jp

* Corresponding author

Keywords:

C₆₀; evaporable fullerene derivatives; organic photovoltaics; organic solar cells; thioketone

Beilstein J. Org. Chem. **2024**, *20*, 1270–1277.
<https://doi.org/10.3762/bjoc.20.109>

Received: 21 February 2024

Accepted: 06 May 2024

Published: 31 May 2024

This article is part of the thematic issue "Carbon-rich materials: from polyaromatic molecules to fullerenes and other carbon allotropes".

Guest Editor: Y. Yamakoshi



© 2024 Zhai et al.; licensee Beilstein-Institut.
License and terms: see end of document.

Abstract

Evaporable indano[60]fullerene ketone (FIDO) was converted to indano[60]fullerene thioketone (FIDS) in high yield by using Lawesson's reagent. Three compounds with different substituents in *para* position were successfully converted to the corresponding thioketones, showing that the reaction tolerates compounds with electron-donating and electron-withdrawing substituents. Computational studies with density functional theory revealed the unique vibrations of the thioketone group in FIDS. The molecular structure of FIDS was confirmed by single-crystal X-ray analysis. Bulk heterojunction organic solar cells using three evaporable fullerene derivatives (FIDO, FIDS, C₆₀) as electron-acceptors were compared, and the open-circuit voltage with FIDS was 0.16 V higher than that with C₆₀.

Introduction

Fullerene is a carbon allotrope that has attracted significant scientific interest since its discovery by H. W. Kroto in 1985 [1]. Due to their distinctive spherical structure and electron-

deficient properties, fullerene derivatives have found applications in various fields, including photovoltaics [2-5], biomedicine [6-8], and electron transporters [9,10]. Organic photo-

voltaic (OPV) and perovskite solar cell (PSC) technologies have proven to be promising candidates for the sustainable use of solar energy, with power conversion efficiency (PCE) improving to 17% for OPVs and over 25% for PSCs in just a few years [11]. Functionalized fullerene derivatives have played an important role both in OPVs as electron acceptors and in PSCs as electron transport layers (ETLs) by efficiently accepting electrons and hindering the transport of holes [12–14].

During the past 10 years, considerable attention has been focused on functional fullerene derivatives with an emphasis on tuning solubility and energy levels. Meanwhile, less attention has been devoted to improving the thermal stability of fullerene derivatives. One well-known example is [6,6]-phenyl-C₆₁-butyric acid methyl ester (PCBM), which is recognized for its excellent solubility in solution-processed OPV fabrication [15]. Films generated through vacuum deposition, on the other hand, exhibit superior quality, have fewer defects, and are eco-friendlier than films produced by spin-casting. However, only a few studies to date have investigated the design of fullerene derivatives with the aim of improving their thermal stability, and more specifically, of designing evaporable fullerene derivatives [16–18]. Recently, we reported on perovskite solar cells fabricated with indano[60]fullerene ketone (FIDO), which was synthesized through fullerene cation chemistry. These cells demonstrated long-term stability and a remarkable PCE of 22.11%, surpassing that of the commonly used C₆₀ (20.45%). This improved performance can be attributed to the evaporated amorphous film, which prevents the transformation of the film into a crystalline state during the heating and aging of the devices. Additionally, the ketone structure acts as a Lewis base, resulting in a passivation effect on Pb²⁺ [19].

In this study, we designed and synthesized indano[60]fullerene thioketones (FIDSs) with various *para*-substituents. The vacuum-deposition performance and thermal stability of FIDS were assessed by both normal-pressure and vacuum thermogravimetric analysis (TGA). Additionally, we conducted a comparative analysis of bulk heterojunction (BHJ) organic solar cells using the three evaporable fullerene derivatives investigated in this work.

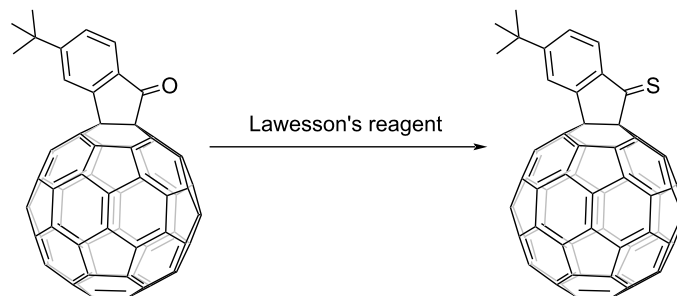
Results and Discussion

The synthesis of FIDO was performed by fullerene cation chemistry as reported by our group [20–26]. Conversion from ketone to thioketone is usually achieved by using Lawesson's reagent, which tends to form a trimer structure when reacted with indanone without a substituent at the α position [27–29]. Introduction of fullerene at the α position facilitated the successful transformation of ketone to thioketone.

Initially, we adopted the widely reported reaction conditions with 1.5 equiv of Lawesson's reagent and tetrahydrofuran (THF) as solvent. *t*-Bu-FIDO was dissolved in THF by sonication for 30 min. Unfortunately, the results were not fully satisfactory. Considering the poor solubility of fullerene derivatives, toluene, carbon disulfide (CS₂), and *ortho*-dichlorobenzene (*o*-DCB) were tested as solvent. Surprisingly, the conversion from ketone to thioketone did not occur as anticipated. In another attempt, where the amount of Lawesson's reagent was increased to 3 equiv (Table 1, entry 5), the signal of thioketone was observed for the first time by high-performance liquid chromatography (HPLC) and MALDI time-of-flight mass spectrometry. Subsequently, a conversion of 99% was achieved by further increasing the amount of Lawesson's reagent and the reaction temperature. The transformation from ketone to thioketone was confirmed by ¹³C NMR, which showed a downfield shift from 198 ppm for the carbonyl carbon to 235 ppm for the thiocarbonyl carbon. With the optimized conditions (Table 1, entry 9) in hand, different *para*-substituents were used and the reaction from FIDO to FIDS was found to tolerate both electron-donating and -withdrawing functional groups as shown in Table 2.

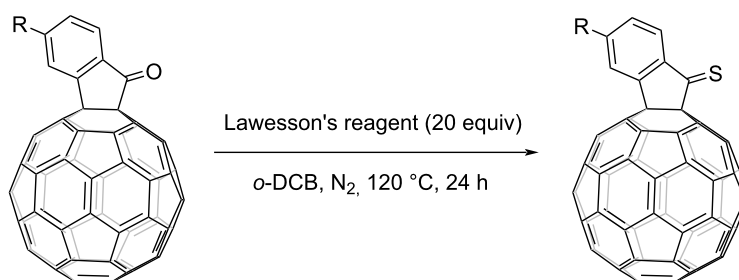
It is well known that functional groups with larger steric hindrance can reduce intermolecular forces. Consequently, a *tert*-butyl-functionalized compound (*t*-Bu-FIDS) was chosen for further studies in this work. To identify the formation of the thiocarbonyl group, Fourier transform infrared spectroscopy (FTIR) was conducted as shown in Figure 1a. The carbonyl stretching vibration peak of *t*-Bu-FIDO at 1720 cm⁻¹ disappeared, indicating all the *t*-Bu-FIDO was completely consumed. Interestingly, the characteristic vibration peak of thiocarbonyl groups was not observed, which should be located at 1050–1300 cm⁻¹ theoretically. Instead, numerous new low-intensity peaks were observed in this region.

To gain a comprehensive understanding of the differences between *t*-Bu-FIDO and *t*-Bu-FIDS, the density functional theory (DFT) method was employed using the B3LYP hybrid functional. The 6-31G* basis set was used for the geometry optimization and frequency calculation. The thiocarbonyl group in FIDS was found to have an out of plane bending vibration, however, the carbonyl group in FIDO showed a strong in-plane stretching vibration as shown in Figure S1 (Supporting Information File 1). Due to the direct connection between the five-membered ring and the fullerene cage, the out of plane bending vibration was easily affected by the fullerene cage vibration. Furthermore, the out-of-plane bending vibration of the thiocarbonyl group was also watched, which also affected the vibration of fullerene cage and benzene ring (Figure S2 and Table S1, Supporting Information File 1). This interesting phenome-

Table 1: Optimization of reaction conditions for the treatment of *t*-Bu-FIDO with Lawesson's reagent.^a

Entry	Equiv	Reaction temperature (°C)	Solvent	Reaction time (h)	Conversion ^b (%)
1	1.5	70	THF	14	NR ^c
2	1.5	50	CS ₂	14	NR
3	1.5	70	<i>o</i> -DCB	14	NR
4	1.5	100	toluene	14	NR
5	3	100	toluene	14	5
6	3	120	toluene	14	10
7	14	120	toluene	14	50
8	20	120	toluene	14	70
9	20	120	toluene	20	90
10	20	120	<i>o</i> -DCB	20	99

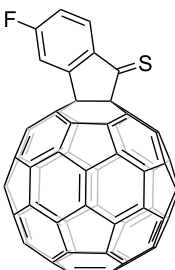
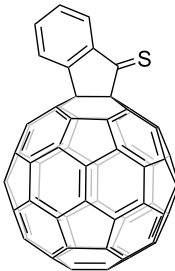
^aAll reactions were performed with *t*-Bu-FIDO (50 mg) under N₂ atmosphere. All the solvents (10 mL) were anhydrous. ^bConversion was estimated from the HPLC peak area ratio. ^cNR = no reaction.

Table 2: Reaction of R-FIDO with Lawesson's reagent.^a

R = H, F, *t*-Bu

Entry	R	Product	Yield ^b (%)	Conversion (%)
1	<i>t</i> -Bu		45	99

Table 2: Reaction of R-FIDO with Lawesson's reagent.^a (continued)

2	F		50	90
3	H		38	95

^aAll reactions were performed in *o*-DCB at 120 °C for 20 h under N₂ atmosphere with FIDO as starting material. The molar ratio of Lawesson's reagent to FIDO was 20:1. ^bIsolated yield.

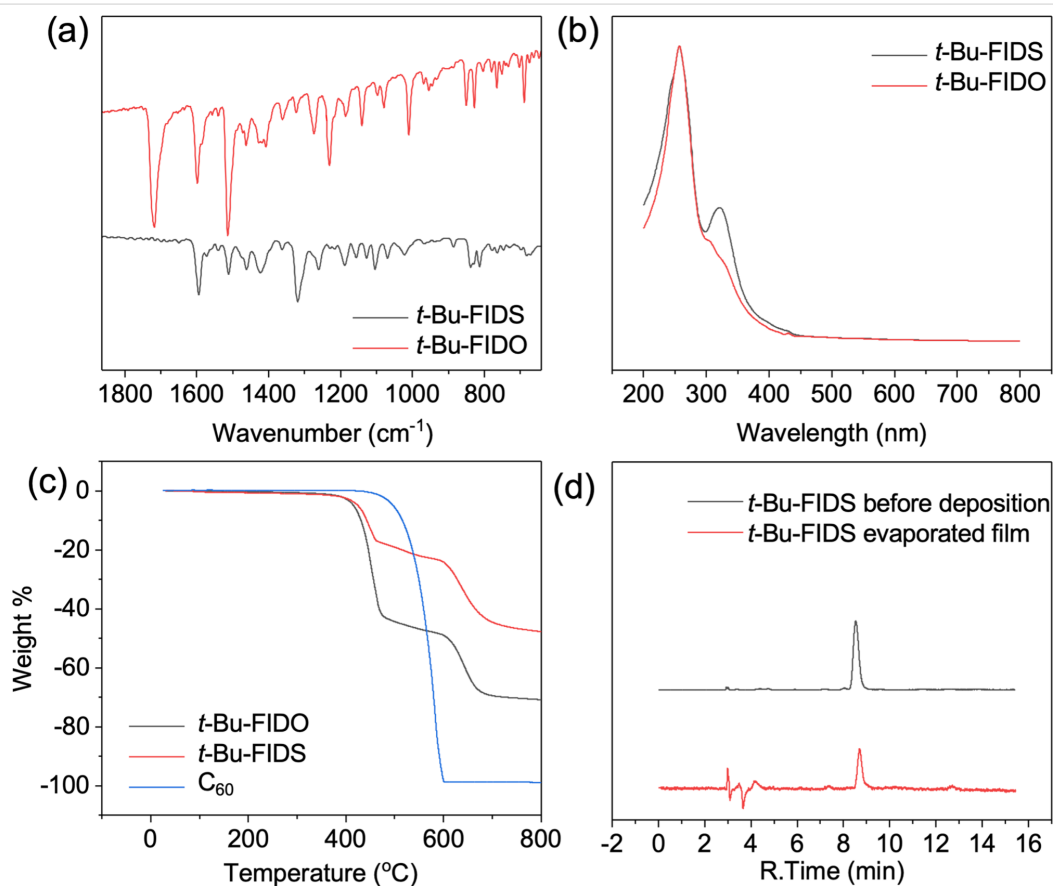


Figure 1: Characterization data. (a) FTIR spectra of *t*-Bu-FIDO and *t*-Bu-FIDS. (b) UV-vis spectra of fullerene derivatives normalized at 270 nm. (c) Vacuum TGA curves of *t*-Bu-FIDO (black), *t*-Bu-FIDS (red), and C₆₀ (blue). The measurements were conducted under 0.1 Pa. (d) HPLC analyses before deposition of *t*-Bu-FIDS (black) and of toluene used to rinse the evaporated film of *t*-Bu-FIDS (red).

non may explain the numerous new peaks that formed around 1000 cm^{-1} for *t*-Bu-FIDS.

Ultraviolet–visible (UV–vis) spectroscopy of *t*-Bu-FIDS in *o*-DCB exhibited two prominent UV absorption bands with peaks at 257 nm and 320 nm (Figure 1b). The absorption at 257 nm indicated the integrity of the fullerene cage chromophore. The absorption peak at 320 nm was assigned to the charge transfer band of the C=S bond in *t*-Bu-FIDS, which was stronger than that of the C=O bond in *t*-Bu-FIDO [30]. Interestingly, the maximum absorption band observed in *t*-Bu-FIDO at 432 nm, which is a characteristic feature of 58π -fullerene derivatives with a 1,2-addition pattern, was absent in *t*-Bu-FIDS [31]. Its absence might be due to perturbation caused by the presence of the C=S bond in *t*-Bu-FIDS.

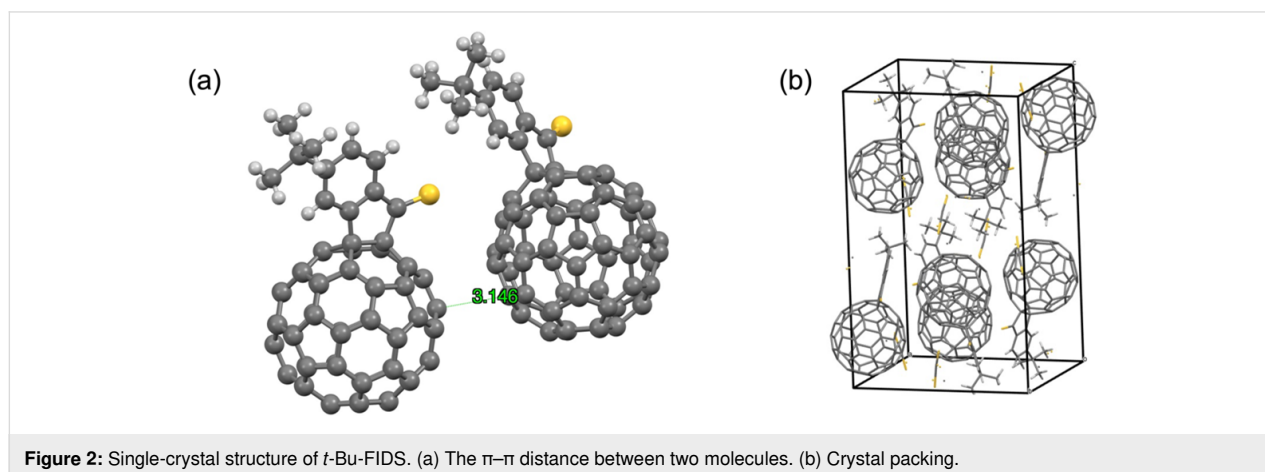
To examine the sublimation behavior of *t*-Bu-FIDS under an environment similar to vacuum deposition, vacuum TGA measurements were performed using a TGA instrument connected to a vacuum pump and heater. The internal pressure of heater was reduced to 0.1 Pa or lower. Figure 1c shows the weight loss of the three fullerene derivatives under vacuum conditions. In contrast to C_{60} , both *t*-Bu-FIDO and *t*-Bu-FIDS exhibited similar two-stage weight-loss curves. The sublimation temperature (T_{sub}) was determined by analyzing the onset of weight loss for these compounds. T_{sub} was lower for *t*-Bu-FIDO and *t*-Bu-FIDS, at 410 °C and 417 °C, respectively, than for C_{60} , which began to sublime at 460 °C (Table 3). The lower sublimation temperature was attributed to the steric hindrance of the *tert*-butyl groups, which disrupted the π – π stacking between the fullerene cages. The slight difference in sublimation temperature between *t*-Bu-FIDO and *t*-Bu-FIDS might be due to the slightly higher electron density of the sulfur atom compared with the oxygen atom. Additionally, data on the degradation temperature (T_{deg}) obtained by normal-pressure TGA are shown in Table 3 and Figure S3 (Supporting Information File 1). T_{deg}

was higher than T_{sub} for all three compounds, indicating their evaporability. Unfortunately, however, the sublimation window ($T_{\text{deg}} - T_{\text{sub}}$) of *t*-Bu-FIDS was narrower than that of *t*-Bu-FIDO due to the lower T_{deg} of *t*-Bu-FIDS. A *t*-Bu-FIDS film was prepared by vacuum deposition at 0.1 Å/s, as shown in Figure 1d and Figure S4 (Supporting Information File 1). The film was uniform and smooth, with a thickness of approximately 20 nm. The film was rinsed with toluene, and the collected toluene was analyzed by HPLC to check for thermal decomposition during vacuum deposition. The *t*-Bu-FIDS structure remained almost unchanged, but very small amounts of two decomposed products were found at retention times of 7.5 min and 12.5 min. The latter decomposed product is C_{60} , judged from the retention time.

Table 3: Sublimation and degradation temperatures of three evaporable fullerene derivatives.

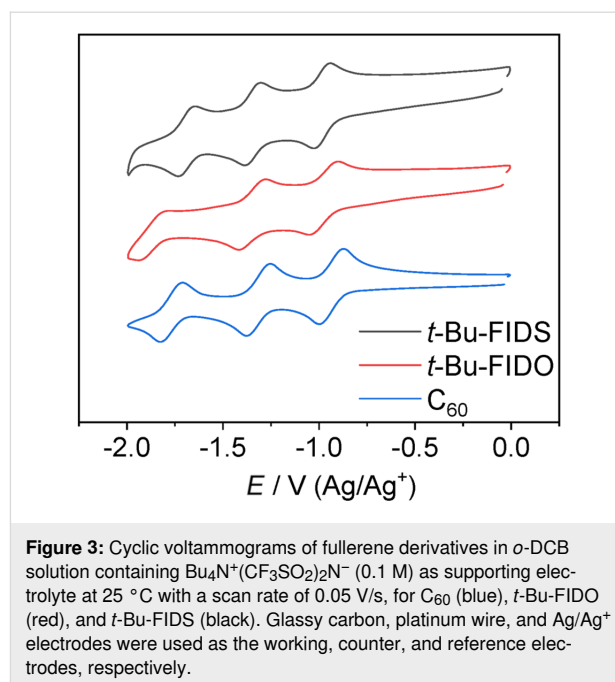
Compound	T_{sub} (°C)	T_{deg} (°C)
C_{60}	460	–
<i>t</i> -Bu-FIDO	410	474
<i>t</i> -Bu-FIDS	417	450

A single crystal of *t*-Bu-FIDS was grown by liquid–liquid diffusion method ($CS_2/EtOH$). The crystal structure was successfully analyzed using synchrotron radiation at SPring-8. The crystal exhibited the orthorhombic space group (No. 61) with the D_{2h} point group, and the structure confirmed the 1,2-addition pattern of *t*-Bu-FIDS (Figure 2a,b). The shortest π – π distance between the two fullerene molecules of *t*-Bu-FIDS in a unit cell was 3.14 Å, while that in *t*-Bu-FIDO was 2.974 Å [19]. The C=S bond length was 1.627 Å and was clearly longer than the C=O bond in *t*-Bu-FIDO. We consider that this longer bond length may have caused the higher reactivity and lower degradation temperature of *t*-Bu-FIDS compared with *t*-Bu-FIDO.



Electron-accepting ability is one of the most important properties for fullerene derivatives, and it is typically described in terms of the energy level of the lowest unoccupied molecular orbital (LUMO). To understand the electron affinity of *t*-Bu-FIDS, cyclic voltammetry was conducted. The cyclic voltammogram of *t*-Bu-FIDS in *o*-DCB showed reversible reduction waves at $E_{1/2} = -1.14$ V and -1.51 V (vs Fc/Fc⁺), as shown in Figure 3. Both the first and second reduction potentials of *t*-Bu-FIDS were higher than those of pristine C₆₀. The LUMO energy of *t*-Bu-FIDS and C₆₀ was calculated as -3.62 eV and -3.68 eV, respectively, using the following equation: $E(\text{LUMO}) = -(E_{1/2}^{\text{red1}} + 4.80)$ eV. To compare the electron affinity among the evaporable fullerenes, *t*-Bu-FIDO was also measured in the same solution system and showed a LUMO energy of -3.64 eV, which was slightly deeper than that of *t*-Bu-FIDS.

The use of vacuum-deposited FIDS as the electron transport layer in perovskite solar cells is still being explored. Considering that the open-circuit voltage (V_{OC}) of OPVs is mainly determined by the difference between the HOMO level of the donor and the LUMO level of the acceptor, *t*-Bu-FIDS, with a higher LUMO level than C₆₀, was used to fabricate a solution-processed BHJ OPV device with the donor poly(3-hexylthio-



phene) (P3HT). For comparison, the two known evaporable fullerenes C₆₀ and *t*-Bu-FIDO were chosen. The results are summarized in Figure 4 and Table 4. Benefiting from higher V_{OC} ,

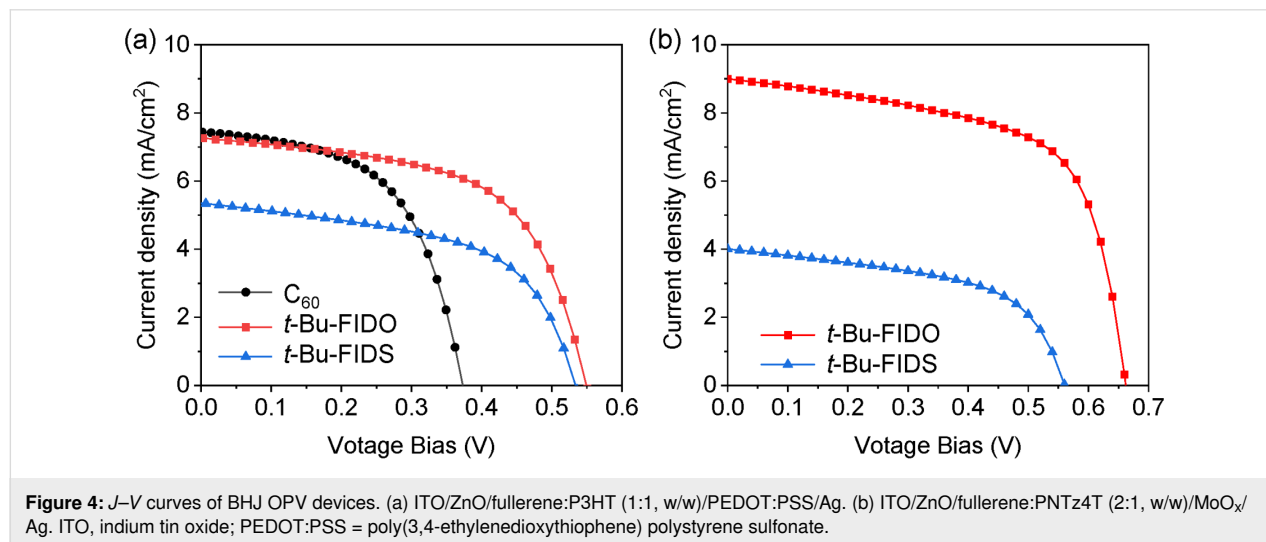


Figure 4: J - V curves of BHJ OPV devices. (a) ITO/ZnO/fullerene:P3HT (1:1, w/w)/PEDOT:PSS/Ag. (b) ITO/ZnO/fullerene:PNTz4T (2:1, w/w)/MoO_x/Ag. ITO, indium tin oxide; PEDOT:PSS = poly(3,4-ethylenedioxythiophene) polystyrene sulfonate.

Table 4: Summary of photovoltaic parameters of BHJ OPV devices.

Fullerene	Donor	V_{OC} (V)	J_{SC} (mA/cm ²)	FF	PCE %
C ₆₀	P3HT ^a	0.37	7.45	0.55	1.55
<i>t</i> -Bu-FIDO	P3HT	0.55	7.53	0.60	2.47
<i>t</i> -Bu-FIDS	P3HT	0.53	5.39	0.55	1.58
<i>t</i> -Bu-FIDO	PNTz4T ^b	0.66	9.00	0.62	3.71
<i>t</i> -Bu-FIDS	PNTz4T	0.56	4.00	0.54	1.23

^aITO/ZnO/fullerene P3HT (1:1, w/w)/PEDOT:PSS/Ag. ^bITO/ZnO/fullerene:PNTz4T (2:1, w/w)/MoO_x/Ag.

the *t*-Bu-FIDS showed a PCE comparable to that of C₆₀, although the short-circuit current density (J_{SC}) was slightly lower. To further improve the performance of *t*-Bu-FIDO and *t*-Bu-FIDS, the crystalline polymer donor PNTz4T [32] was used. Compared with *t*-Bu-FIDS, *t*-Bu-FIDO achieved 3.71% PCE with larger J_{SC} and higher V_{OC} . With PNTz4T, *t*-Bu-FIDS exhibited low performance, with J_{SC} of only 4 mA/cm². This lower V_{OC} may be attributable to a suboptimal BHJ structure between PNTz4T and *t*-Bu-FIDS. Considering the lower J_{SC} performance of *t*-Bu-FIDS with both P3HT and PNTz4T, *t*-Bu-FIDS might not be suitable for BHJ OPV devices.

Conclusion

In summary, we successfully synthesized evaporable indano[60]fullerene thioketones with functional groups at the *para*-position of the benzene ring. Furthermore, we examined the sublimation behavior of three evaporable fullerene derivatives (FIDO, FIDS, C₆₀). The sublimation window of *t*-Bu-FIDS was unfortunately slightly narrower than that of *t*-Bu-FIDO, which we have previously reported. Additionally, we compared the solution-processed OPV performance of the three evaporable fullerene derivatives as electron acceptors. FIDO exhibited the best performance, with V_{OC} that was 0.18 V higher compared with C₆₀. Although FIDS showed a lower performance due to its less-desirable BHJ structure in the OPV, it could still potentially be utilized in perovskite solar cells in the future.

Supporting Information

Supporting Information File 1

Experimental procedures, device fabrication, method of single-crystal growth, device evaluations and characterizations.

[<https://www.beilstein-journals.org/bjoc/content/supplementary/1860-5397-20-109-S1.pdf>]

Supporting Information File 2

Chemical information file of *t*-Bu-FIDS, CCDC deposition number 2332797.

[<https://www.beilstein-journals.org/bjoc/content/supplementary/1860-5397-20-109-S2.cif>]

Funding

This work was financially supported by the Japan Society for the Promotion of Science (JSPS) KAKENHI Grant Numbers 21KK0087 and 23H05443. Y.M. thanks the Takahashi Industrial and Economic Research Foundation and the Yashima Environment Technology Foundation for financial support. This

work was supported by the Japan Science and Technology Agency (JST SPRING), Grant Number JPMJSP2125. The synchrotron radiation experiment was performed at Spring-8 with the approval of the Japan Synchrotron Radiation Research Institute (JASRI) (Proposal No. 2023A1758).

ORCID® iDs

Shinobu Aoyagi - <https://orcid.org/0000-0002-7393-343X>

Tsubasa Mikie - <https://orcid.org/0000-0003-0532-8905>

Takeshi Igarashi - <https://orcid.org/0000-0002-3621-6335>

Yutaka Matsuo - <https://orcid.org/0000-0001-9084-9670>

Data Availability Statement

The data that supports the findings of this study is available from the corresponding author upon reasonable request.

References

- Kroto, H. W.; Heath, J. R.; O'Brien, S. C.; Curl, R. F.; Smalley, R. E. *Nature* **1985**, *318*, 162–163. doi:10.1038/318162a0
- Yu, G.; Gao, J.; Hummelen, J. C.; Wudl, F.; Heeger, A. J. *Science* **1995**, *270*, 1789–1791. doi:10.1126/science.270.5243.1789
- Matsuo, Y. *Chem. Lett.* **2012**, *41*, 754–759. doi:10.1246/cl.2012.754
- Lin, H.-S.; Matsuo, Y. Fullerenes in Photovoltaics. In *Handbook of Fullerene Science and Technology*; Lu, X.; Akasaka, T.; Slanina, Z., Eds.; Springer Nature: Singapore, 2022; pp 851–888. doi:10.1007/978-981-16-8994-9_37
- Matsuo, Y.; Kawai, J.; Inada, H.; Nakagawa, T.; Ota, H.; Otsubo, S.; Nakamura, E. *Adv. Mater. (Weinheim, Ger.)* **2013**, *25*, 6266–6269. doi:10.1002/adma.201302607
- Friedman, S. H.; DeCamp, D. L.; Sijbesma, R. P.; Srdanov, G.; Wudl, F.; Kenyon, G. L. *J. Am. Chem. Soc.* **1993**, *115*, 6506–6509. doi:10.1021/ja00068a005
- Martinez, Z. S.; Castro, E.; Seong, C.-S.; Cerón, M. R.; Echegoyen, L.; Llano, M. *Antimicrob. Agents Chemother.* **2016**, *60*, 5731–5741. doi:10.1128/aac.00341-16
- Bakry, R.; Vallant, R. M.; Najam-ul-Haq, M.; Rainer, M.; Szabo, Z.; Huck, C. W.; Bonn, G. K. *Int. J. Nanomed.* **2007**, *2*, 639–649.
- Abe, Y.; Tanaka, H.; Guo, Y.; Matsuo, Y.; Nakamura, E. *J. Am. Chem. Soc.* **2014**, *136*, 3366–3369. doi:10.1021/ja500340f
- Lenoble, J.; Campidelli, S.; Maringa, N.; Donnio, B.; Guillon, D.; Yevlampieva, N.; Deschenaux, R. *J. Am. Chem. Soc.* **2007**, *129*, 9941–9952. doi:10.1021/ja071012o
- Wang, D. H.; Park, K. H.; Seo, J. H.; Seifert, J.; Jeon, J. H.; Kim, J. K.; Park, J. H.; Park, O. O.; Heeger, A. J. *Adv. Energy Mater.* **2011**, *1*, 766–770. doi:10.1002/aenm.201100347
- Heo, J. H.; Han, H. J.; Kim, D.; Ahn, T. K.; Im, S. H. *Energy Environ. Sci.* **2015**, *8*, 1602–1608. doi:10.1039/c5ee00120j
- Lin, X.; Cui, D.; Luo, X.; Zhang, C.; Han, Q.; Wang, Y.; Han, L. *Energy Environ. Sci.* **2020**, *13*, 3823–3847. doi:10.1039/d0ee02017f
- Yu, Z.; Yang, Z.; Ni, Z.; Shao, Y.; Chen, B.; Lin, Y.; Wei, H.; Yu, Z. J.; Holman, Z.; Huang, J. *Nat. Energy* **2020**, *5*, 657–665. doi:10.1038/s41560-020-0657-y
- Ganesamoorthy, R.; Sathiyam, G.; Sakthivel, P. *Sol. Energy Mater. Sol. Cells* **2017**, *161*, 102–148. doi:10.1016/j.solmat.2016.11.024
- Shibuya, H.; Suk Choi, Y.; Choi, T.; Yun, S.; Moon, J.; Matsuo, Y. *Chem. – Asian J.* **2022**, *17*, e202200609. doi:10.1002/asia.202200609

17. Matsuo, Y.; Ishikawa, S.; Amada, H.; Yokoyama, K.; Shui, Q.-j.; Huda, M.; Ueoka, N.; Lin, H.-S. *Chem. Lett.* **2023**, *52*, 685–687. doi:10.1246/cl.230217
18. Lin, H.-S.; Ma, Y.; Xiang, R.; Manzhos, S.; Jeon, I.; Maruyama, S.; Matsuo, Y. *Commun. Chem.* **2021**, *4*, 74. doi:10.1038/s42004-021-00511-4
19. Shui, Q.-J.; Shan, S.; Zhai, Y.-C.; Aoyagi, S.; Izawa, S.; Huda, M.; Yu, C.-Y.; Zuo, L.; Chen, H.; Lin, H.-S.; Matsuo, Y. *J. Am. Chem. Soc.* **2023**, *145*, 27307–27315. doi:10.1021/jacs.3c07192
20. Yang, X.-Y.; Lin, H.-S.; Matsuo, Y. *J. Org. Chem.* **2019**, *84*, 16314–16322. doi:10.1021/acs.joc.9b02618
21. Lin, H.-S.; Jeon, I.; Chen, Y.; Yang, X.-Y.; Nakagawa, T.; Maruyama, S.; Manzhos, S.; Matsuo, Y. *Chem. Mater.* **2019**, *31*, 8432–8439. doi:10.1021/acs.chemmater.9b02468
22. Lin, H.-S.; Matsuo, Y. *Chem. Commun.* **2018**, *54*, 11244–11259. doi:10.1039/c8cc05965a
23. Yang, X.-Y.; Lin, H.-S.; Jeon, I.; Matsuo, Y. *Org. Lett.* **2018**, *20*, 3372–3376. doi:10.1021/acs.orglett.8b01295
24. Matsuo, Y.; Ogumi, K.; Zhang, Y.; Okada, H.; Nakagawa, T.; Ueno, H.; Gocho, A.; Nakamura, E. *J. Mater. Chem. A* **2017**, *5*, 2774–2783. doi:10.1039/c6ta10319g
25. Zhang, Y.; Matsuo, Y.; Nakamura, E. *Org. Lett.* **2011**, *13*, 6058–6061. doi:10.1021/ol202511u
26. Zhang, Y.; Matsuo, Y.; Li, C.-Z.; Tanaka, H.; Nakamura, E. *J. Am. Chem. Soc.* **2011**, *133*, 8086–8089. doi:10.1021/ja201267t
27. Campaigne, E.; Moss, R. D. *J. Am. Chem. Soc.* **1954**, *76*, 1269–1271. doi:10.1021/ja01634a020
28. Rufanov, K. A.; Stepanov, A. S.; Lemenovskii, D. A.; Churakov, A. V. *Heteroat. Chem.* **1999**, *10*, 369–371. doi:10.1002/(sici)1098-1071(1999)10:5<369::aid-hc5>3.0.co;2-z
29. Ozturk, T.; Ertas, E.; Mert, O. *Chem. Rev.* **2007**, *107*, 5210–5278. doi:10.1021/cr040650b
30. Pandey, M.; Muthu, S.; Nanje Gowda, N. M. *J. Mol. Struct.* **2017**, *1130*, 511–521. doi:10.1016/j.molstruc.2016.10.064
31. Varotto, A.; Treat, N. D.; Jo, J.; Shuttle, C. G.; Batara, N. A.; Brunetti, F. G.; Seo, J. H.; Chabinyk, M. L.; Hawker, C. J.; Heeger, A. J.; Wudl, F. *Angew. Chem., Int. Ed.* **2011**, *50*, 5166–5169. doi:10.1002/anie.201100029
32. Vohra, V.; Kawashima, K.; Kakara, T.; Koganezawa, T.; Osaka, I.; Takimiya, K.; Murata, H. *Nat. Photonics* **2015**, *9*, 403–408. doi:10.1038/nphoton.2015.84

License and Terms

This is an open access article licensed under the terms of the Beilstein-Institut Open Access License Agreement (<https://www.beilstein-journals.org/bjoc/terms>), which is identical to the Creative Commons Attribution 4.0 International License (<https://creativecommons.org/licenses/by/4.0>). The reuse of material under this license requires that the author(s), source and license are credited. Third-party material in this article could be subject to other licenses (typically indicated in the credit line), and in this case, users are required to obtain permission from the license holder to reuse the material.

The definitive version of this article is the electronic one which can be found at: <https://doi.org/10.3762/bjoc.20.109>